MONOTONIC AND NONMONOTONIC AREA PRESERVING MAPS, AND RELATED BIFURCATIONS IN LASER ACCELERATOR

L. G. Brunnet[a], G. Corso[b] and F. B. Rizzato[a]
[a]IF–UFRGS, P.O.Box 15051 91501-970 Porto Alegre, RS, Brasil
[b]IF–USP, P.O.Box 66318 053389-970, São Paulo, SP, Brasil

Abstract

In this paper we analyze the behavior of area preserving maps and related bifurcations in an accelerator system as a function of the tuning involving orbital and external wave frequencies. It is found out that while sharp tuning leads to nonmonotonic maps, poor tuning leads to monotonic maps. The transition between these two situations and the associated sequences of bifurcations are studied in detail.

————————-

The purpose of this paper is to compare sequences of Hamiltonian bifurcations preceding chaos in weakly and strongly resonant wave-particle interactions. The terms weak and strong refer to the magnitude of the frequency mismatch between wave and relativistically-shifted particle frequencies; weak means large mismatches and strong, small mismatches.

In the model, a relativistic particle is simultaneously submitted to the action of a background magnetic field pointing along the z axis and an electrostatic harmonic wave propagating along the x axis. The corresponding adimensional Hamiltonian can be written as [1]-[2]

$$H = [1 + P_x^2 + (P_y + x)^2 + P_z^2]^{1/2} + A_o \cos(kx - \omega t). \quad (1)$$

With the normalizations adopted the wave frequency ω and $c\,k$ are both measured in units of the electron-cyclotron frequency.

Taking $P_y = 0$, introducing canonical guiding center coordinates, $P_x = \sqrt{2I} \cos \theta$, $x = \sqrt{2I} \sin \theta$, and making use of the harmonic expansion for Bessel functions, it becomes possible to cast the Hamiltonian in the resonant form [3]-[7]

$$H = H_o(I) + A_o \sum_{l=-\infty}^{+\infty} J_l(k\sqrt{2I}) \cos(l\theta + (l-1)\,\omega t) \quad (2)$$

where $H_o \equiv [1 + 2I + P_z^2]^{1/2} - \omega I$ and where the $l = 1$ resonance has been conveniently rendered time independent by means of usual canonical transformations. Hamiltonian (2) generates a set of primary resonances $I_{(n,n-1)}$, $n = +1, +2, +3...$, that can be located along the action axis I of the appropriate gyro phase-space according to relation $n|\omega_o(I_{(n,n-1)})| = (n-1)\,\omega$. For higher order islands a positive integer m may appear on the right-hand side replacing $(n-1)$ in the form $n|\omega_o(I_{(n,p)})| = m\omega$, $m/n < 1$; we shall refer to the ratio m/n as the winding of the island chain. Specializing the discussion on cyclotronic wave frequencies

$\omega = 1$ from now on, one notes that the most important influence in the low energy region $I \sim 0$ comes from the $(1,0)$-resonance. Its salient role is a result of the associated Bessel factor which is much larger than those of other resonances there; indeed, one has $J_1(2\sqrt{I})/J_n(2\sqrt{I}) \sim 1/I^{(n-1)/2} \gg 1$ if $I \ll 1$.

Let us then analyze the $(1,0)$-resonance in some more detail. The appropriate resonant Hamiltonian can be written in the form:

$$H_{(1,0)} = \delta I - \eta I^2 + A_o \frac{\sqrt{2I}}{2} \cos \theta, \quad (3)$$

where besides $\omega = 1$ we have also set $k = 1$, recalling that $I \ll 1$.

Examining Hamiltonian (3) we point out that an effective negative mismatch δ is introduced when $P_z > 0$. If δ is sufficiently small, island saturation is governed by the balance involving the nonlinear η-term and the Bessel function term. In this case which we call strongly resonant in view of the smallness of the mismatch term, saturation is relativistic since the nonlinear term comes from relativistic mass corrections [1, 5]. In the weakly resonant case where δ is large, island saturation is nonrelativistic because it is commanded by the linear δ-term.

In any case, the maximum amplitude of the $(1,0)$-resonance can be obtained by setting $\theta = H_{(1,0)} = 0$ in (3); the last equality, in particular, defines the boundary trajectory, i.e. the trajectory dividing trapped from untrapped orbits in the gyro phase-space. The maximum amplitude of weakly resonant islands (quadratic terms discarded), can be thus estimated as $I_{wr} = (1/2)(A_o/\delta)^2$ and the amplitude of strongly resonant islands (δ term discarded) as $I_r = (1/2)^{1/3}(A_o/\eta)^{2/3}$. This leads to conclude that saturation is weakly resonant with I_{wr} dominating over I_r, $I_{wr} \ll I_r$, when $A_o \ll A_*(P_z) \equiv 2^{1/2}(\delta^{3/2}/\eta^{1/2})$; the reverse situation takes place when $A_o \gg A_*(P_z)$.

1.1 Strong Resonance

In the strongly resonant case one can approximately set $P_z \to 0$ and obtain some analytical results [2]. It has been shown that in this case the tuning character is nonmonotonic. Starting from the central elliptic point of island $(1,0)$ and moving towards $I \to \infty$, the frequency first decreases as one goes towards the boundary and then increases as one crosses the boundary and proceeds beyond.

1.2 Weak Resonance

In the weakly resonant regime, one can perform a Lie perturbative theory to estimate the frequency behavior inside the $(1, 0)$-island [2]. In this second case the system can be seen as displaying a monotonic tuning character where the frequency is always increasing as one moves towards $I \to \infty$ starting from the central elliptic point.

_____

In both cases, the frequency at the boundary can be shown to be non-zero. This remarkable fact leads to unusual inverse saddle-node bifurcation at and close to this location.

2.1 Strongly Resonant Bifurcations

Consider the strongly resonant regime first, that is, the non-monotonic case. The frequency is larger at the elliptic point, decreases as one approaches the boundary and starts to increase again as $I \to \infty$. Now, as one increases the wave amplitude a chain internal to the $(1, 0)$-resonance with winding $[r, s]$ (symbol "( )" denotes originally external chains and "[ ]" denotes internal chains) is born at the central elliptic point when the amplitude is such that $r|\omega_e| = s\omega$. Considering the shape of the frequency curve and the fact that the whole curve displaces upwards as the wave amplitude increases, the chain start to migrate towards the boundary arriving there at the same time as the boundary touches an external chain with the same winding. Then, a inverse saddle node bifurcation is likely to occur.

2.2 Weakly Resonant Bifurcations

In the weakly resonant case, the situation changes. In view of the fact that the tuning character is purely monotonic there can be no simultaneous presence of internal and external chains with the same winding; this point has not been made clear in previous works [2]. Since in this case the gyrofrequency decreases as one approaches the central elliptic point, as the wave amplitude grows an originally external (m, n) chain is engulfed by the expanding boundary, becomes thereafter an internal chain, moves towards the central elliptic point, and eventually vanishes there when the wave amplitude A_o is such that $m\omega_e = n\omega$.

3 THE GENERAL CASE

The question which has not yet been properly analyzed in the literature, refers to what happens with the external chain if one is operating in the neighborhood of the transition from weak to strong resonant regimes. What is likely to happen in this case is that the external chain collapses against an internal chain *after* the former has crossed the boundary but *before* it reaches the central elliptic point. Let us see if this is what really happens.

We use $P_z = 0.4$ to illustrate this transition case. As predicted above, the external chain crosses the $(1, 0)$-boundary but *do not* arrive at the central elliptic point, undergoing the inverse saddle-node *before* that. Fig. (1) displays the gyro
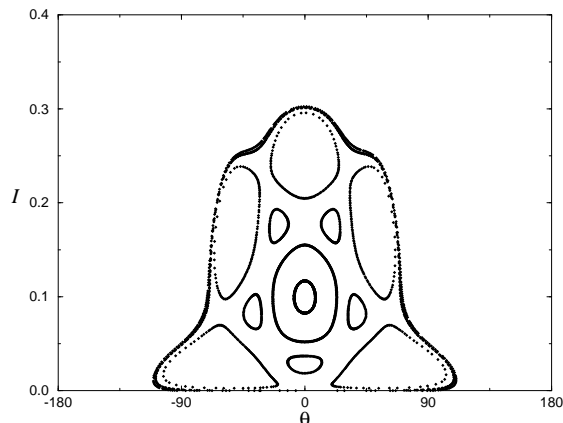

Figure 1: Poincaré surface of sections for $A_o = 0.125$ and $P_z = 0.4$.

phase-space for the $P_z = 0.4$ case. The outermost chain is the originally external $p = 5$-chain and the innermost is a $[5, 1]$-chain produced at the central elliptic point. The figure represents the dynamics just before the saddle node. Fig. (2) represents the dynamics at saddle node; for a slightly larger value of A_o than that of Fig. (4b), the external elliptic points also vanish. We emphasize that the saddle-node takes place *inside* the $(1, 0)$-boundary which is the curve connecting $(I = 0, \theta = -\pi/2)$ to $(I = 0, \theta = \pi/2)$, but much after the external island has chance to arrive at the central fixed point.
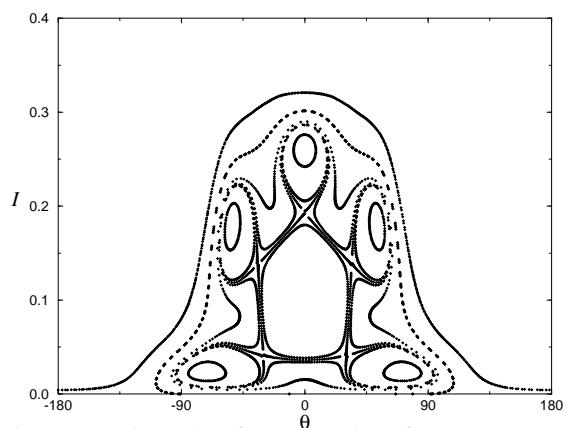

Figure 2: Poincaré surface of sections for $A_o = 0.1255$ and $p_z = 0.4$

The calculations performed in this paper indicate that the position of saddle-node bifurcations in accelerating systems are sensitive on the value of the injected beam momentum P_z. In addition to previous analysis for large and small values of P_z we have found here that in intermediary cases external resonances get through the boundary and undergo inverse saddle-node before they reach the central elliptic point.

4 ACKNOWLEDGMENTS

5   REFERENCES

[1] R.C. Davidson, Y.-T. Yang and R.E. Aamodt, J. Plasma Phys. **41** (1989) 405.

[2] G. Corso and F.B. Rizzato, Physica **D 80**, 296 (1995); and Phys. Rev. E **52 52**, 3591 (1995).

[3] A. J. Lichtenberg and M. A. Lieberman, Regular and Stochastic Motion, (Springer, Berlin, 1983).

[4] B. Chirikov, Phys. Rep. **52** (1979) 263.

[5] T.S. Caetano, F. Couto, R. Pakter, G. Corso, L.G. Brunnet, and F.B. Rizzato, Chaos, Solitons & Fractals **7**, 165 (1996).

[6] G.A. Oda and I.L. Caldas, Chaos, Solitons & Fractals, **5** 15 (1995).

[7] J. E. Howard and J. Humphreys, Physica **D 80**, 265 (1995).